Electron and Proton Transfer on the Acceptor Side of the Reaction Center in Chromatophores of *Rhodobacter capsulatus*: Evidence for Direct Protonation of the Semiquinone State of Q_B[†]

Jérôme Lavergne,* Cédric Matthews, and Nicolas Ginet

CEA-DEVM/LBC, Cadarache, 13108 Saint Paul-lez-Durance, France

Received November 20, 1998; Revised Manuscript Received January 20, 1999

ABSTRACT: 1. The absorption changes associated with the formation of $P^+Q_B^{red}$ (Q_B^{red} stands for the semiquinone state of the secondary quinone acceptor) were investigated in chromatophores of *Rhodobacter capsulatus*. Marked modifications of the semiquinone spectrum were observed when the pH was lowered from 7 to 5. These modifications match those expected for a complete conversion of Q_B^{red} from the anionic state Q_B^- at pH 7 to the neutral protonated state Q_BH at pH 5. Similar modifications were observed in chromatophores from *Rb. sphaeroides*, but not in purified reaction centers from *Rb. capsulatus*, suggesting that the environment of the reaction center (native membrane vs detergent micelle) is the crucial parameter. 2. The recombination reaction $P^+Q_B^{red} \rightarrow PQ_B$ was investigated as a function of pH. No particular kinetic heterogeneity was observed at low pH, showing that Q_BH remains mostly bound to the reaction center. The rate constant reaches a minimum value of 0.08 s^{-1} at pH 6, suggesting that the direct route for recombination prevails in chromatophores below this pH, instead of the usual pathway via Q_A^-. 3. The proton uptake caused by Q_B^{red} is about 1 below pH 7 and decreases at higher pH. It is suggested that the pH dependence of the conversion of Q_B^- to Q_BH, occurring in a range where the uptake is constant, cannot be accommodated by a purely electrostatic model, but probably involves a conformational change. 4. The kinetics of the electron-transfer reaction $Q_A^-Q_B \rightarrow Q_AQ_B^{red}$ were investigated. A 2-fold acceleration was observed between pH 7 and pH 5 ($t_{1/2} \approx 30$ and 15 μs, respectively). A fast ($\ll$10 μs) unresolved phase appears to be present at both pHs. The second electron-transfer $Q_A^-Q_B^{red} \rightarrow Q_AQ_BH_2$ proceeds with a similar rate as the first electron transfer (15−30 μs phase). Consequences for the rate-limiting step are discussed. 5. The carotenoid shift, indicative of the membrane potential, displays a rising phase concomitant with the $Q_A^-Q_B \rightarrow Q_AQ_B^{red}$ electron transfer. Its relative extent is markedly increased at pH 5, with part of the kinetics occurring during the unresolved fast phase. 6. The extent of the electrochromic shift of bacteriopheophytin around 750 nm associated with formation of Q_B^{red} decreases toward acidic pH, reflecting the charge compensation due to proton uptake and the formation of neutral Q_BH.

A central mechanism in bioenergetics is the coupling of electron and proton transfer, which is the origin of the Mitchellian protonmotive force used for ATP synthesis. An increasingly detailed knowledge of this process has been gained in recent years about the acceptor side of bacterial reaction centers [see reviews (*1*, *2*)]. The formation of ubiquinol in the Q_B[1] pocket of the reaction center requires two photochemically driven reduction steps. The first one results in the formation of a semiquinone: $Q_A^-Q_B \rightarrow Q_AQ_B^-$, where Q_A is the primary quinone acceptor and Q_B a more loosely bound ubiquinone, taken up from the lipid-soluble pool. The semiquinone Q_B^- is a stable state which remains attached to the protein pocket until the second reduction step: $Q_A^-Q_B^- + 2\ H^+ \rightarrow Q_A\ Q_BH_2$. The doubly reduced, doubly protonated quinol Q_BH_2 is then released from the Q_B pocket and exchanged against an oxidized quinone. A similar mechanism occurs on the acceptor side of the photosystem II reaction center in oxygenic photosynthesis.

The current view (*2*−*4*) about proton transfer during this process may be outlined as follows. The first step (formation of Q_B^-) is accompanied by substoichiometric proton binding to amino acid residues, which undergo a p*K* shift due to the electrostatic influence of the anionic semiquinone. The second step involves first the transient formation of the doubly reduced, singly protonated state Q_BH^-, followed by the binding of the second proton and release of the quinol. A number of spectroscopic studies (*5*−*7*) have established the anionic character of the semiquinone Q_B^-, over the accessible pH range [down to pH 6 (*8*)]. The above picture, however, has been derived essentially from studies on purified, detergent-solubilized reaction centers. One reason for studying reaction centers embedded in detergent micelles rather than in the native membrane environment is, of course, the important signal-to-noise improvement for spectroscopic measurements brought about by purification. Another advantage is that the three-dimensional structure derived from crystallography pertains to the same type of material. One

[†] This work was supported by the CEA and the CNRS.

* Address correspondence to this author (E-mail: lavergne@dsvcad.cea.fr).

[1] Abbreviations: Bph, bacteriopheophytin; Cyt, cytochrome; P, primary donor; Q_A, primary quinone acceptor; Q_B, secondary quinone acceptor; Q_B^{red}, semiquinone state of Q_B (anionic or protonated); RC, reaction center; TMPD, *N*,*N*,*N*′,*N*′-tetramethyl-1,4-phenylenediamine; UQ, ubiquinone-10.

10.1021/bi9827621 CCC: $18.00
Published on Web 03/19/1999

should not, however, lose sight of the fact that the physiologically relevant object is a membrane protein and that some caution may be necessary when extending knowledge gained from the isolated RC to the native system. It has been known, for instance, that significant differences exist between purified and membrane-inserted reaction centers, concerning the acceptor side kinetics and their pH-dependence (*9*, *10*). In this paper, we further investigate electron and proton transfer on the acceptor side of the RC in chromatophores, and show that, at variance with isolated RCs, direct protonation of the semiquinone takes place below pH 7.

MATERIALS AND METHODS

Bacterial Strains. Rb. capsulatus FJ2, a kind gift of Prof. F. Daldal, was derived from a green strain (MT1131) and deleted in both cytochrome c_2 and the alternative membrane-bound cytochrome c_y (*11*). We also used a similar double mutant of *Rb. sphaeroides* 2.4.1, CYC17 (a kind gift of Prof. Donohue), that was deleted in cytochromes c_2 and iso-c_2 (*12*). This strain still contains a membrane-bound cytochrome c_y which is not operative for RC reduction. These nonphotosynthetic strains were grown aerobically in darkness in Hutner medium supplemented with the antibiotics (spectinomycin and kanamycin) corresponding to the resistance cassettes associated with the deletions.

Chromatophores. The cells, suspended in MOPS, 50 mM, pH 7.0, and KCl, 50 mM, were broken through a French press (11 000 psi). Unbroken cells were eliminated by centrifugation (17000*g*, 15 min), and the supernatant was spun at 200000*g* for 90 min. The chromatophore pellet was resuspended in a medium containing 0.5 mM MOPS, pH 7.0 (a low buffer concentration was used to allow measurement of flash-induced pH changes), 50 mM KCl, and 25% v/v glycerol. Aliquots of the suspension were kept frozen at − 80 °C. For experiments, the thawed samples were diluted 10−40 times (depending on the spectral region investigated) in a medium containing 50 mM KCl and (except for pH change measurements) 50 mM buffer (MES, HEPES, or TRIS depending on the pH).

Isolated reaction centers from WT *Rb. capsulatus*, prepared as in reference (*13*), were a kind gift of Dr. L Baciou.

Spectroscopic Measurements. We used a laboratory-built Joliot-type (*14*, *15*) spectrophotometer. This machine offers a high sensitivity [rms noise/transmitted light = $(2-4) \times 10^{-5}$ on a single run] due to the use of sparse, but intense, short (2 μs) monochromatic flashes for the detecting beam. The signal is corrected for the energy fluctuations of the individual flashes, measured in an optically identical reference path. Single-turnover actinic excitation was provided by a xenon flash lamp (2 μs width at half-peak) filtered through a near-IR Kodak Wratten 89B filter. Alternatively, the 100 ns pulses from an alexandrite laser could be used (λ = 780 nm). The measuring photodiodes were protected from the scattered actinic light and from bacteriochlorophyll fluorescence by a broad blue filter (Schott BG-39), except for running experiments in the 700−850 nm region where measurements could not be made earlier than 1 ms after the actinic flash. In the near-UV region, we used the conversion device previously described (*16*). A piece of white paper soaked with glycerol is inserted against the incident side of the blue filter. The "whiteners" contained in the paper act as efficient converters of the light absorbed in the 290−370 nm region into fluoresced visible light, which is transmitted by the blue filter. This system eliminates the problem presented by UV filters of a transmission window in the near-IR, causing fluorescence artifacts. With these filter combinations, in the visible and UV region, the actinic flash caused negligible perturbation and no dead time was required before triggering the first detecting flash. To minimize the contribution of short-lived triplet signals, we chose 10 μs as the shortest delay between the actinic flash and the first measuring flash.

For the measurement of proton uptake, we monitored the absorption changes of pH-sensitive dyes at 586 nm, where the background absorption change (in the absence of the dye, or after adding a buffer) is essentially zero. The following dyes were used: bromocresol purple (pH 5−6.5), cresol red (pH 6.5−8.5) at concentrations of 10−25 μM. Valinomycin (3 μM) was present.

RESULTS

Spectra of $P^+Q_B^{red}$ as a Function of pH. To study Q_B^- absorption changes in chromatophores or cells, it may be a useful simplification to eliminate any donor side reaction. In the absence of a secondary donor to P^+, the flash-induced reactions are restricted as schematized below (omitting submicrosecond reactions):

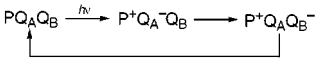

In this system, Q_B^- is formed less than 1 ms after the flash and disappears in the seconds time range through a recombination with P^+. If Q_B^- were initially present in a fraction of centers, formation and release of quinol would occur rapidly following the flash, so that P^+ would be left without a reducing partner. If this long-lived P^+ eventually is reduced, the center is reset to the PQ_B state (whereas if P^+ remains oxidized, the center is photochemically inactive). Therefore, preillumination of the system cannot lead to any significant accumulation of state PQ_B^-, unless the redox conditions are sufficiently reducing to cause chemical reduction of Q_B to Q_B^-. Genetically engineered mutants bearing deletion of the native donors to P^+ (such as strain FJ2 of *Rb. capsulatus*, which was used in most of the present work) provide a material completely devoid of donor side reactions. The use of such a material that allows one to deal with only two states (on the millisecond−second time scale) is of particular advantage for studying the UV-blue part of the spectrum where all known efficient donors to P^+ interfere spectrally.

Figure 1A shows the spectra in the UV-blue region of the absorption changes of FJ2 chromatophores measured a few milliseconds after a flash, for two values of the pH. These spectra were normalized to the same initial amount of P^+ (correcting slight concentration variations of individual samples), measured as the difference 542 nm − 603 nm. The vertical scale was computed by assuming for this difference an extinction coefficient of 30 mM^{-1} cm^{-1} (*17*).[2] Due to the presence of valinomycin, the flash-induced membrane potential and the associated absorption changes decay in less than 1 ms, so that the spectra of Figure 1A are entirely due to the difference ($P^+Q_B^-$ − PQ_B). Marked differences are observed between the spectra recorded at pH

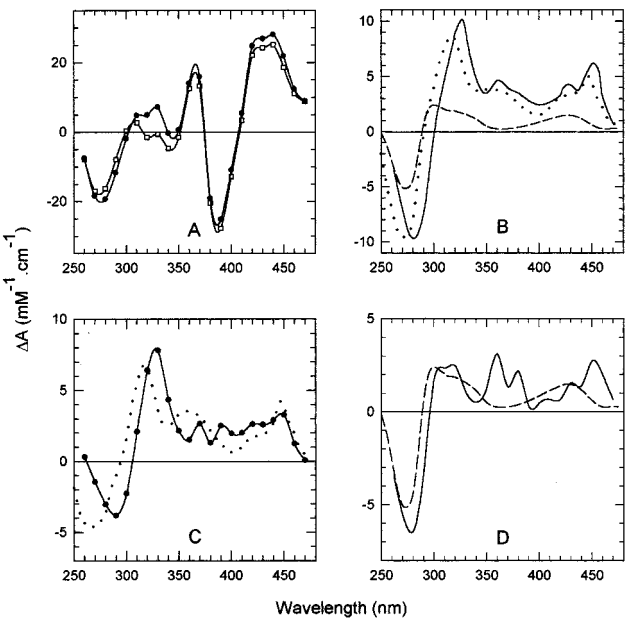

FIGURE 1: Panel A: spectra of ($P^+Q_B^{red}-PQ_B$) at pH 7.3 (solid circles) and pH 5.0 (open squares). The absorption changes were measured 3 ms after the flash. The medium contained 3 μM valinomycin. Panel B: dotted and dashed curves, spectra replotted (with permission) from the data of Bensasson and Land (1973)-(*18*) for UQ_{10} in methanol; dotted line, difference (UQ^- − UQ); dashed line, difference (UQH − UQ). The solid curve is the (Q_B^- − Q_B) spectrum for reaction centers of *Rb. sphaeroides*, replotted from (*5*) (with permission), normalized at $\epsilon_{450} = 6.0$ mM^{-1} cm^{-1} [according to (*42*)]. Panel C: solid circles and line, difference (pH 7.3 − pH 5.0) of the spectra of panel A; dotted curve, difference (UQ^- − UQH) of the dotted and dashed curves from panel B. Panel D: dashed line, (UQH − UQ) spectrum (same is in panel B); solid line, double difference ($Q_BH - Q_B^-$) (solid line in panel C) minus (Q_B^- − Q_B) (solid line in panel B), equivalent to ($Q_BH - Q_B$).

7.3 (solid circles) and 5.0 (open squares) in the regions where the spectral features of semiquinone are located. In contrast, these differences show no correlation with the (P^+ − P) spectrum, and we will thus make the assumption that they are at least predominantly due to the acceptor side. The difference between the two spectra, shown in Figure 1C (closed circles), is roughly reminiscent of a (UQ^- − UQ) spectrum and might suggest that a fraction of the semiquinone has somehow disappeared at pH 5. This is not supported, however, by the observed recombination kinetics (see discussion of Figure 5) which indicate the presence of the reducing partner of P^+. The nature of the change occurring to the semiquinone at pH 5 is enlightened by a comparison with the spectra obtained for ubiquinone-10 in methanol by Bensasson and Land (*18*). In panel B are shown the spectra obtained by these authors for (UQ^- − UQ) (dotted line) and for (UQH − UQ) (dashed line), where UQ^- and UQH stand for the anionic and protonated neutral forms of ubisemiquinone, respectively. The solid line shows the (Q_B^- − Q_B) spectrum measured by Verméglio (*5*) in purified RCs, illustrating the shift toward longer wavelengths of the anionic semiquinone spectrum in vivo. The peak and trough for (Q_B^- − Q_B) are located at about 328 and 285 nm, respectively, in reaction centers, and at about 317 and 271 nm, respectively, for (UQ^- − UQ) in methanol. The difference between the dotted and dashed spectra of panel B (i.e., UQ^- − UQH) was plotted in panel C (dotted line). It resembles the spectrum (solid circles) that we obtained in chromatophores for the difference (pH 7.3 − pH 5), especially if one takes into account the wavelength shift between the semiquinone spectra in vitro and in vivo. The present results thus suggest that a significant fraction of Q_B^- is a neutral, protonated semiquinone (UQH) at pH 5, whereas it is anionic at pH 7.3. Furthermore, the finding of similar amplitudes on this extinction coefficient scale for the chromatophore (pH 7.3 − pH 5) spectrum and for the (UQ^- − UQH) spectrum (panel C) suggests that the conversion from anionic to protonated semiquinone is essentially complete when going from pH 7.3 to 5. In other words, the semiquinone must be close to 100% anionic at pH 7.5 and close to 100% protonated at pH 5. This pH-dependent modification of the $P^+Q_B^{red}$ (the notation Q_B^{red} will be used henceforth when the anionic/protonated state of the semiquinone is left unspecified) spectrum was found essentially reversible when first incubating the sample at pH 5, and then raising the pH to 7.

Panel D of Figure 1 shows a comparison of the (UQH − UQ) spectrum (dashed line, same as in panel B) with the spectrum that we ascribe to (Q_BH − Q_B) (solid line, difference between the solid line spectra of panels B and C). The accuracy of the latter is limited because it results from a double difference and also involves different materials (*sphaeroides* RCs and *capsulatus* chromatophores) and a normalization between them. The two spectra of panel D are similar in the 260−350 nm range (apart from the wavelength shift), but differences appear around 370 and 450 nm. In the latter case at least (450 nm peak), we are confident that this difference is significant, based on a special experimental focus. Whereas the conversion from the anionic to protonated form of the semiquinone corresponds to a collapse by about 80% of the 330 nm peak, similar to what is observed in vitro, the 450 nm peak is only diminished by about 55%, much less than in vitro. A consequence of this point is that the 450 nm peak is not as good an indicator of the anionic nature of Q_B^- as the 330 nm peak (or the 330 nm − 290 nm difference used below), at variance with what was usually assumed [see, for instance, (*8*)].

In Figure 2, the extent of the absorbance change difference (330 nm − 290 nm), i.e., the peak *minus* trough of the (Q_B^- − Q_BH) spectrum, for the ($P^+Q_B^{red}$ − PQ_B) absorption change obtained under the same conditions as in the experiment of Figure 1 was plotted as a function of pH (solid circles). This shows that the conversion to the protonated form occurs around an apparent p*K* close to 6. We consistently observed a rise of the curve below pH 5, which may suggest re-formation of anionic semiquinone. On the other hand, this feature may be somehow related to an aggregation of the chromatophores, which we observed for pH <5.

The open circles in Figure 2 are the result of an experiment run with chromatophores from *Rb. sphaeroides* (CYC17) instead of *Rb. capsulatus*. A similar behavior was observed, showing that the formation of Q_BH at low pH is not restricted to *capsulatus*. We also carried out the same measurements using purified reaction centers of *Rb. capsulatus* (open

[2] The chromatophore spectra were not corrected for flattening. This seemed unnecessary since we observed little distortion when comparing ($P^+Q_A^-$ − PQ_A) spectra from chromatophores and isolated reaction centers. A similar conclusion was reached when comparing the overall absorption spectrum of the chromatophore suspension with that of its solubilized pigments [following Pulles (*44*)].

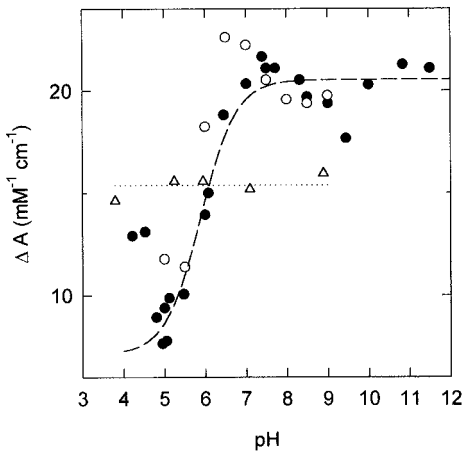

FIGURE 2: Difference of the absorption changes (330 nm − 290 nm) as a function of pH. Same conditions as for Figure 1A. Closed circles, FJ2 chromatophores (the dashed curve is a fit by a Henderson−Hasselbach function of the data for pH ≥5). Open circles, CYC17 chromatophores. Open triangles, purified reaction centers from *Rb. capsulatus*.

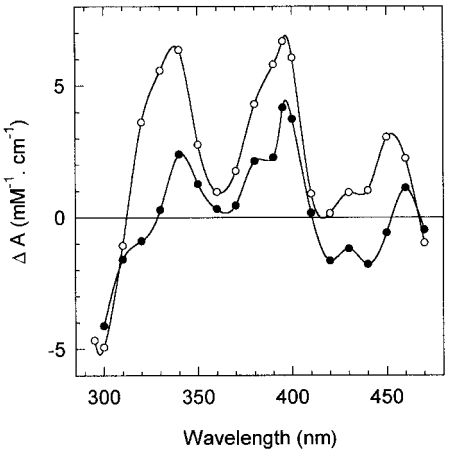

FIGURE 3: Spectra of (Q_A^- − Q_B^{red}) at pH 7.3 (solid circles) and pH 5.0 (open circles). These spectra were obtained by subtracting from the change measured at 3 ms after a flash in the presence of stigmatellin ($P^+Q_A^-$) the change measured in the absence of the inhibitor ($P^+Q_B^{red}$). Valinomycin (3 μM) was present throughout.

triangles). The preparation was dialyzed to exchange LDAO against Triton X-100, to avoid LDAO precipitation at low pH. An excess of UQ_{10} was added, and the presence of the secondary quinone in the Q_B pocket was evidenced by the recombination kinetics. At variance with chromatophores of the same species, no significant change of the UV spectrum (330 nm − 290 nm) of $P^+Q_B^{red}$ was found in the pH range 4−9.[3]

We also investigated the ($P^+Q_A^-$ − PQ_A) spectrum. This absorption change was observed at a few milliseconds after a flash, in the presence of stigmatellin as an inhibitor of electron transfer to Q_B (in this material, stigmatellin was found more efficient than other inhibitors, such as *o*-phenantroline, terbutryn, or atrazine). Some modifications of the ($P^+Q_A^-$ − PQ_A) spectrum were observed between pH 7.5 and 5. These changes were smaller than for the ($P^+Q_B^{red}$ − PQ_B) spectrum, and had no obvious relation with a semiquinone spectrum. By computing the difference between the ($P^+Q_A^-$ − PQ_A) and ($P^+Q_B^{red}$ − PQ_B) spectra, one obtains the spectrum for (Q_A^- − Q_B^{red}), shown in Figure 3 for pH 5 and 7.3. At both pHs, a peak is observed around 395 nm, which cannot be ascribed to a semiquinone feature and is probably due to an electrochromic shift in the Soret band of the bacteriopheophytins. Such shifts have been well characterized for the Q_y band around 750 nm, and we will examine below the effect of pH in this spectral region. At pH 7.3 (solid circles), the other changes around 330 and 450 nm reflect a shift of the Q_B^- spectrum toward shorter wavelengths with respect to that of Q_A^-. This shift was also apparent around the 330 nm peak in the spectra of Verméglio and Clayton (*19*). In the blue region (390−470 nm), our results agree with those recently reported by Li et al. (*20*) for isolated reaction centers. At pH 5 (open circles), the (Q_A^- − Q_B^-) difference spectrum is dominated by the transition from anionic semiquinone Q_A^- to protonated semiquinone Q_BH. The double difference spectrum computed by subtracting the two spectra of Figure 3 (not shown) resembles the (Q_B^- − Q_BH) spectrum of Figure 1C, with distortions due to the pH dependence of the Q_A^- contribution. In particular, such a distortion occurs in the 395 nm region (Bph shift), where the increase of the peak at pH 5 with respect to pH 7.3 is mostly due to Q_A^-.

Proton Uptake. To determine the stoichiometry of proton uptake by Q_B^{red} in FJ2 chromatophores as a function of pH, we monitored the absorption changes of pH-sensitive dyes in the presence of an electron donor to P. We used ferrocene (150 μM) + ferrocyanide (1 mM) as a donor system involving no proton reaction (*21*). Under these conditions, the reduction of P^+ is completed in 200 ms, which is fast compared with the competing recombination reaction. The illumination regime consisted of a series of four flashes spaced 1 s apart, followed by 2−4 min dark-adaptation. This procedure was appropriate for maintaining a close to maximum level of semiquinone oscillations at 450 nm. When lowering the pH, the amplitude of the 450 nm oscillation diminished, because of the modification of the semiquinone spectrum, with no increase of the damping. The oscillation was still detectable at pH 5, in agreement with our finding that the 450 nm band is diminished but not eliminated in fully protonated Q_BH. The dye absorption changes measured under such conditions can give a self-calibrated pattern of proton uptake because, as a first approximation (neglecting the damping), the overall proton uptake on two consecutive flashes should be 2, corresponding to the formation of 1 quinol per RC. This relies, however, on the assumption that there is no other reaction involving protons. We actually found that the oxidized ferrocene was able to mimic the cyt c_2 function, reacting with the $b-c_1$ complex and promoting an electrogenic phase in the 10 ms time range following even-numbered flashes (when quinol is released). This was efficiently inhibited by 1 μM myxothiazol. On the other hand, even in the presence of this inhibitor, a direct cycling occurs in the alkaline pH range, whereby quinol reduces the oxidized ferrocene. This was observed by monitoring ferrocene absorption changes in the UV (oxidized ferrocene accumulates at low pH, but not at high pH). In proton

[3] The data points for isolated RCs (triangles) lie below the level ascribed to 100% anionic semiquinone in chromatophores (i.e., 15 instead of 20). This cannot be ascribed to our neglecting the spectral flattening in chromatophores, which should cause an opposite effect, and must be due to some other spectral difference between the two materials.

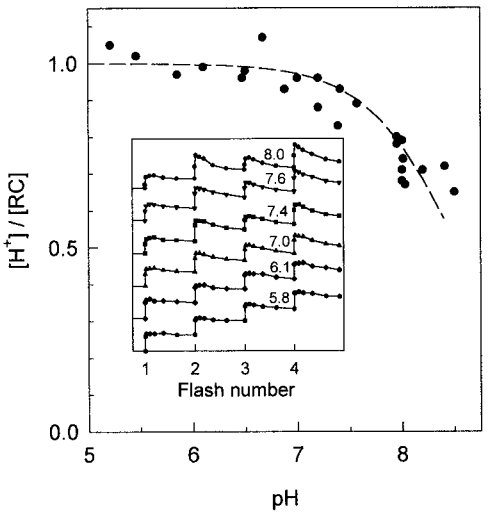

FIGURE 4: Proton uptake by Q_B^{red} as a function of pH. The chromatophores were suspended in a 50 mM KCl medium containing ferrocene (150 μM), ferrocyanide (1 mM), myxothiazol (1 μM), valinomycin (3 μM), and dye (see Materials and Methods). The absorbance changes of the dyes were measured at 586 nm. The uptake on the first flash was computed by assuming a total of 2 H^+/RC on the first and second flashes. The inset shows the traces obtained at various pHs.

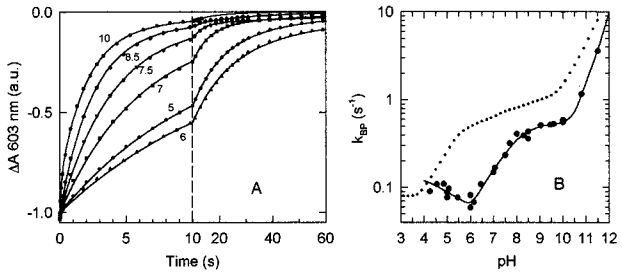

FIGURE 5: Panel A: decay of P^+ following a saturating flash, monitored at 603 nm at various pHs (as indicated). Valinomycin (3 μM) was present. The lines are the result of a fit (see Table 1) with a sum of two (or three at pH 10) exponential components. All traces were normalized to an initial amplitude of -1 for the fitting function. Panel B: rate of P^+ decay as a function of pH. The quantity plotted here is an overall rate constant computed from the half-time of the kinetics, $k_{BP} = \ln(2)/t_{1/2}$. The dotted curve was redrawn (with permission) from the data of Mikšovská et al. (*22*) obtained with isolated RCs of *Rb. capsulatus*.

measurements, this corresponds to acidification kinetics following the uptake, observed after even-numbered flashes. These kinetics become rapid at pH >8.5, truncating the extent of the uptake and precluding in this pH range a reliable use of our calibration method.

The inset in Figure 4 shows the dye responses at various pHs. At low pH, the uptake signal is identical on each flash, whereas at high pH the signal is smaller on odd-numbered flashes and larger on even-numbered ones. The stoichiometry computed from these experiments for the proton uptake caused by semiquinone formation (first flash) is shown in Figure 4. The uptake is close to 1 proton per RC below pH 7. It decreases at higher pH, to about 0.65 H^+ per RC at pH 8.5.

Recombination Kinetics. Figure 5A shows the decay kinetics of P^+ measured at 603 nm at various pHs. Whatever the pH, the kinetics are not well fitted by a single exponential, but rather by a sum of two exponentials, or three at pH 10 (see the half-times and relative amplitudes in Table 1). There

Table 1: Results of Exponential Fits of the Data of Figure 5

pH	$t_{1/2}$ (s)	A (%)	$t_{1/2}$ (s)	A (%)	$t_{1/2}$ (s)	A (%)
5.0	−	−	7.4	81	27	19
6.0	−	−	8.7	74	34	26
7.0	−	−	4.1	90	50	10
7.5	−	−	2.7	94	50	6
8.5	−	−	1.7	90	15	10
10.0	0.09	16	1.3	73	6.7	11

is no indication, however, of any gross kinetic heterogeneity occurring in the pH range where protonation of the semiquinone occurs. At pH 5, the main phase accounts for 80% of the amplitude, and its rate is slowed by less than a factor 2 with respect to pH 7. A very slow phase ($t_{1/2} \geq 25$ s) is present in all curves below pH 7.5. It is almost 2-fold larger at pH 5 than at pH 7. This may indicate a release of the protonated semiquinone from the Q_B site in a minor fraction of the centers. It is nevertheless clear from the family of decay curves in Figure 5 that most centers still undergo a recombination reaction down to pH 5. The changes affecting the semiquinone spectrum in the range of pH 7−5 cannot be due to a disappearance of the semiquinone (e.g., by dismutation), nor to the presence of a large fraction of Q_B^- present in the dark, but must indicate a chemical modification of the semiquinone.

The rate constant for the overall P^+ decay was plotted as a function of pH in Figure 5B. Surprisingly, a minimum is observed at pH 6, and the rate increases slightly at more acidic pH. The upper curve shows, for comparison, the results obtained by Baciou et al. (*13*) with extension to lower pH by Mikšovská et al. (*22*) for isolated reaction centers of *Rb. capsulatus*. The recombination rate is slower in chromatophores by a factor of 2−7, depending on the pH. There is nevertheless a resemblance of the shapes of the two curves, which may be described like a shift by 2−3 units, in the acidic region, of the pH scale for reaction centers with respect to membranes.

$Q_A^-Q_B \rightarrow Q_AQ_B^{red}$ Kinetics. As shown in Figure 3, there are spectral differences between Q_A^- and Q_B^{red} which may be used to monitor the electron-transfer kinetics between the two quinone acceptors. At variance with the experiments described so far, valinomycin was omitted, to avoid possible contributions of changes associated with the membrane potential decay induced by the ionophore in the millisecond or submillisecond range. At pH 5, the reaction involves a change from anionic (Q_A^-) to protonated (Q_BH) semiquinone, so that the spectral differences are relatively large. The kinetics monitored at the 330 nm peak are shown in Figure 6A. Within experimental accuracy, the decay is fitted by a single exponential with $t_{1/2} \approx 15$ μs. Panel B shows the results obtained in the presence of ferrocene, on the first and second flashes. The reduction of P^+ by ferrocene at the concentration used (25 μM) occurs in the hundred millisecond range, i.e., slow with respect to the time scale of Figure 6, but fast with respect to $P^+Q_B^{red}$ recombination. The kinetics observed for the first electron transfer (formation of a semiquinone at Q_B) and for the second one (formation of quinol) have very similar rates.

It was expected that the kinetics in the absence of donor, or in the presence of ferrocene for the first flash, should be identical. There is, however, a significant difference between the data of panel A and the first flash curve of panel B:

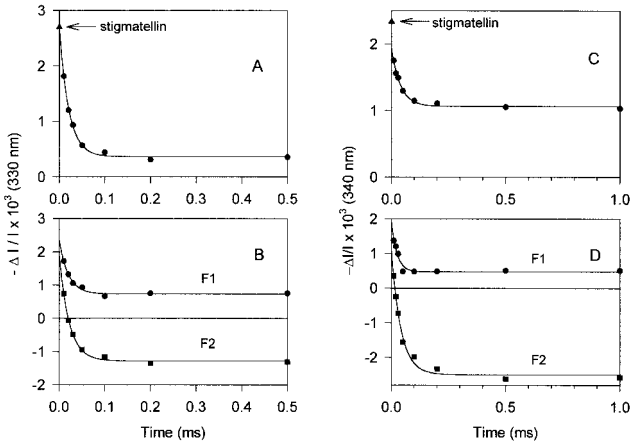

FIGURE 6: Kinetics of electron transfer from Q_A to Q_B, at pH 5.0 (A and B) or pH 7.2 (C and D). In panels A and C, no donor was present. In panels B and D, 25 μM ferrocene was added, and two successive flashes (spaced 1s apart) were fired on a dark-adapted sample (F1 and F2 indicate the kinetics following the first and second flash, with respect to a base line measured before each flash). In panels A and C, the level measured in the presence of stigmatellin (7 μM) is indicated. The absorbance changes were measured at 330 nm in panels A and B, and at 340 nm in panels C and D. The lines are results of fits with a single-exponential decay. In panels A and B, the best fits for all three curves had a similar half-time ($t_{1/2} = 15 \pm 1$ μs). Such was also the case for the three curves in panels C and D ($t_{1/2} = 28 \pm 1$ μs).

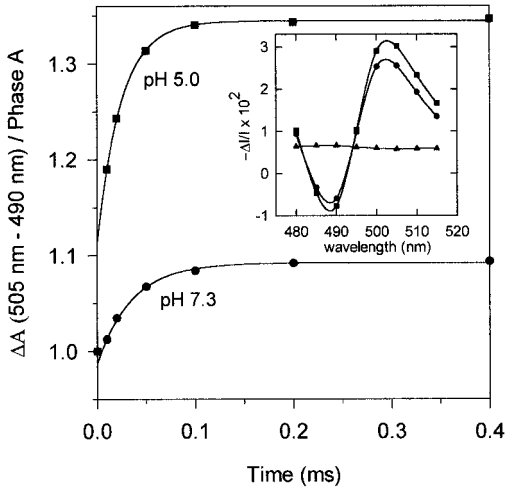

FIGURE 7: Kinetics of the carotenoid shift at pH 7.3 and pH 5.0, following a laser flash. The difference of the absorption changes at 505 and 490 nm was normalized with respect to the same difference measured in the presence of stigmatellin, at 10 μs (phase A = 1). The triplet correction (measured as explained in the text) was about 0.015 at 10 μs. The inset shows the spectra recorded at pH 6.0 for phase A (circles, 10 μs, stigmatellin present) and for phase A + phase B (squares, 30 ms, no inhibitor). The triangles show the P^+ contribution measured in the presence of valinomycin.

whereas the decay rate is about the same, the extent of the change is smaller in panel B. In other words, it seems that semiquinone is not any more entirely protonated (at pH 5) but partly anionic. This effect is caused by ferrocene and develops continuously during the incubation with this substance. At pH 6 or 7 (see panels C and D), ferrocene causes an opposite modification, apparently increasing the fraction of protonated semiquinone. These ferrocene-induced modifications of absorption changes monitored in the submillisecond time scale can hardly be due to an electron-transfer reaction involving ferrocene directly since, as mentioned above, the reduction of P^+ takes place on a much slower range. These effects were observed as well when the sample was kept in the dark during the whole incubation period and cannot be due to preillumination. A similar effect (at pH 5) was observed with potassium ferricyanide at low concentration (a few micromolar), but, surprisingly, not with ferrocyanide (although the reduced form could be expected to be the active one, as for ferrocene).

At pH 7.2, there is almost no absorption change at 330 nm during the electron transfer from Q_A to Q_B, but other wavelengths can be used (Figure 3). The kinetics monitored at 340 nm are shown in Figure 6C,D. The reaction is about 2-fold slower than at pH 5, with $t_{1/2} \approx 28$ μs. Again, the same rate is observed for the first and second electron-transfer steps in the presence of ferrocene.

In Figure 6A,C are indicated the absorption change measured in the presence of stigmatellin, i.e., for $P^+Q_A^-$. If stigmatellin does not affect the spectrum of Q_A^-, this level should indicate the initial value of the kinetics (the initial extent of P^+, measured at 603 nm, was not modified by stigmatellin). In the experiment of Figure 6A (330 nm, pH 5), it is close to the level extrapolated at time zero for the exponential fit. This is not true, however, in the case of Figure 6C (340 nm, pH 7.2), where the extrapolation at time zero lies significantly below the stigmatellin level. This suggests the occurrence of an unresolved fast phase completed in less than 10 μs. At pH 5, whereas this fast phase was very small at 330 nm, it could be detected at other wavelengths (e.g., 340 nm, and in the carotenoid shift bands; see below).

Electrogenic Phases. The electric field across the membrane causes an electrochromic shift of the carotenoid absorption spectrum that can be used to monitor electrogenic events (*23*). It is known that an increase of the membrane potential ("phase BI") accompanies the electron transfer from Q_A to Q_B (*24*). We measured the kinetics of the absorption changes for the difference (505 nm − 490 nm). These wavelengths are close to the peak and trough of the carotenoid shift in a "green" strain, and the difference eliminates almost completely the $P^+Q_B^-$ contribution (essentially due to P^+). A short-lived signal is observed after the flash due to formation of triplet carotenoid (*25*). The amplitude of this signal was estimated by monitoring the changes caused by a flash triggered a short time (e.g., 15 ms) after a saturating preflash, so that essentially all RCs are in the $P^+Q_B^-$ state, unable to perform charge separation. These changes should thus essentially be due to triplet carotenoid. This procedure may somewhat overestimate the triplet signal occurring when the flash addresses a dark-adapted sample, because in this case a fraction of the photons are used up for photochemical charge separation. When using a xenon flash, the triplet caused a significant contribution for about 40 μs. This is longer than the true lifetime of the triplet (a few microseconds) because the "tail" of the flash extends the duration of triplet formation. When using a 100 ns laser flash, with slightly undersaturating energy, the triplet correction was small at 10 μs and negligible at longer times. Figure 7 shows the kinetics recorded under such conditions at pH 5.0 and 7.3. The changes were normalized to the level measured at 10 μs in the presence of stigmatellin (reflecting the electrogenicity of the $P^+Q_A^-$ state, "phase A").

The magnitude of the carotenoid shift (e.g., of phase A) was smaller, relative to the P^+ signal, at pH 5 compared with neutral pH, and its spectrum was slightly shifted toward shorter wavelengths. This decrease continued during the incubation at low pH, and the data shown in Figure 7 (pH 5) were corrected for this drift. At variance with the $P^+Q_B^{red}$ spectrum, the modification of the carotenoid shift at low pH was irreversible; i.e., the size of the signal was not restored when raising the pH to 7.5.

The kinetics of Figure 7 were fitted with single-exponential functions, yielding similar half-times (17 and 24 μs at pH 5 and 7.3, respectively) as for the UV changes of Figure 6. At low pH, besides the acceleration, a considerable increase in the relative extent of the kinetics is observed. Also, the extrapolation of the kinetics to time zero lies markedly above the stigmatellin level at pH 5 (presence of an unresolved rapid phase), whereas such is not the case at pH 7.3. The relative overall rise above the stigmatellin level was found in the range of 35−45% at pH 5 and 9−11% at pH 7.3. We checked that the absorption changes observed in the 480−515 nm region on the time scale of Figure 7 matched the spectrum of the carotenoid shift. This is illustrated by the inset of Figure 7 showing the spectra measured at 10 μs in the presence of stigmatellin (phase A) or in the absence of inhibitor in the 10 ms range (phase A + phase B).

In the presence of stigmatellin, we observed small (about 3% of the total amplitude) decreasing kinetics of the carotenoid shift occurring with a similar rate as the kinetics observed in the absence of the inhibitor (for the rise of the carotenoid shift or 340 nm kinetics). This result (only investigated at pH 7.3) agrees with those obtained by Brzezinsky (*26*) using a photovoltage technique.

Bacteriopheophytin Shift. The absorption changes associated with the formation of Q_A^- or Q_B^{red} comprise, besides specific semiquinone bands, electrochromic contributions in the near-infrared due to their electrostatic influence on nearby pigments (mainly BPh_A for Q_A^-, BPh_B for Q_B^{red}) (*9*, *10*, *19*). In the case of Q_B^{red}, this part of the spectrum is expected to depend on the degree of electrostatic compensation exerted by proton uptake, especially when direct protonation of the semiquinone is involved. In this spectral region, there is no problem with the use of an artificial donor like TMPD which does not contribute to absorption changes (ferrocene could also be used but was avoided because of its effects on the semiquinone state described above). This allows us to obtain a pure ($Q_B^- - Q_B$) spectrum devoid of the P^+ contribution which is large in this region. Figure 8 shows the spectra thus obtained at various pHs for the first flash on a dark-adapted sample, measuring the absorption change at 400 ms, after total reduction of P^+ by TMPD. The amplitude of the spectra (normalized to the same amount of initial P^+) was markedly dependent on the pH.

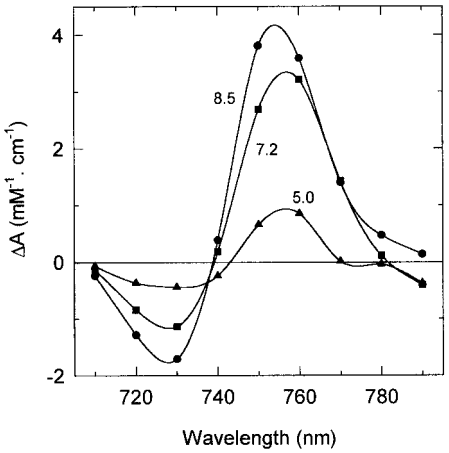

FIGURE 8: Near-infrared spectra of Q_B^{red} at various pHs, as indicated. The absorption changes were measured at 400 ms after a flash, following complete reduction of P^+ by TMPD (300 μM). KCN (5 mM) was added to slow the autoxidation of TMPD.

DISCUSSION

Protonation of Q_B^{red}. Our proposal of direct protonation of the semiquinone Q_B^{red} at low pH in chromatophores relies on the following arguments. First, a major spectral change is observed in the UV bands of the semiquinone when lowering the pH. This change matches the difference predicted from in vitro data for the conversion of the anionic semiquinone to the neutral, protonated form. The shape of this difference spectrum is not, however, drastically different from a ($UQ^- - UQ$) spectrum, so that one may consider the alternative possibility of a diminished amount of Q_B^- at low pH. The extent of the observed change would imply a loss of more than half the Q_B^- at pH 5 with respect to pH 7. For a given initial amount of $P^+Q_A^-$, a diminished amount of $P^+Q_B^-$ might originate from a fraction of Q_B^- being present in the dark-adapted state. In this fraction of centers, the electron transfer would result in quinol formation, and the contribution to the observed spectral change would be that of ($Q_BH_2 - Q_B^-$). In our chromatophores devoid of a donor to P^+, this fraction of centers should be blocked in the P^+ state because the recombination partner has been removed. A very biphasic time course for the reduction of P^+ should thus appear specifically when lowering the pH, which was not observed (Figure 5). A slow component with $t_{1/2} \approx 27$ s accounts for 20% of the P^+ decay at pH 5 but also for 10% at pH 7. One would also expect some kind of binary oscillation on successive flashes (e.g., different kinetics after a first or second flash) if some Q_B^- were initially present, which was not observed either. Another possibility could be that low pH favors some pathway for dismutation, where Q_B^- from two centers would, directly or not, interact and yield one quinol and one quinone. The above arguments based on the recombination kinetics still apply against this hypothesis, and also the fast (15 μs) decay kinetics of the 330 nm peak at pH 5, which hardly fits a mechanism involving interaction between the Q_B^- located in different RCs.

The unorthodox finding of protonation of Q_B^{red} prompted us to examine whether this was a characteristic of chromatophores in general, or of the species. Using purified reaction centers from *Rb. capsulatus*, we found, in agreement with previous literature [(*8*) for the pH range 9.5−6], that the Q_B^- spectrum remains unmodified down to pH 4. On the other hand, using chromatophores from *Rb. sphaeroides*, we obtained a decrease of the 330 nm − 290 nm difference at low pH, similar to that observed with *capsulatus* chromatophores. We thus conclude that the critical parameter is the membrane vs detergent micelle environment of the RC. It may be useful to recall that the p*K* of semi-UQ_{10} is about 6.5 in methanol (*27*), so that our finding of an apparent p*K*

of about 6 is not in itself a particular surprise.[4] The surprise is rather the difference between chromatophores and solubilized RCs. In the latter case, we observed no significant protonation down to pH 4 so that the p*K* of the semiquinone must be less than 3, thus at least 3 units below the chromatophore value. This raises the following question: Can such a difference be accounted for purely by electrostatic effects due to the solvent, or are there structural changes between the two materials? In the following, we give several arguments supporting the latter possibility.

The full transition from anionic to protonated semiquinone takes place between pH 7 and 5. It could be accommodated by a Henderson−Hasselbach equation with p*K* around 6. On the other hand, it is actually surprising to observe this type of dependence where a steep transition occurs within 2 pH units, because of the interactions between protonatable residues around the Q_B pocket. The proton uptake is close to 1 at pH 7 (and below). At this pH, Q_B^{red} is still anionic, and, thus, one or several residues, strongly interacting with Q_B^- (which is also a protonatable group), must be responsible for the uptake. The interaction between protonatable groups is expected to cause a delocalization of the proton on several sites and to spread on a broad pH range the protonation of an individual group [see, for instance, (*28*) for an experimental titration of Glu L-212, and (*29, 30*) for computational approaches]. It should be noted, however, that, at variance with these results, the effect of the L 212-Glu→Gln mutation on proton uptake does not support such a broad titration range for Glu L-212 (*22, 31*). From attempts at modelization of the present problem, we believe that it is not possible to account, even roughly, for the experimental features (constant proton uptake of 1 below pH 7 *and* titration of the semiquinone protonation localized entirely between pH 7 and 5) with a purely electrostatic model. By "purely electrostatic model", we mean a fixed distribution of groups with given intrinsic p*K*s and pairwise electrostatic interactions.[5] Therefore, our results instead suggest a conformational change occurring around pH 6 which would affect the Q_B pocket so as to render the direct protonation of Q_B^{red} energetically favorable. The titration wave observed around pH 6 might then reflect the conformational switch rather than the p*K* of Q_B^-.[6] The conformational change required to account for the present observations need not be of a large extent. According to the crystallographic studies of Stowell et al. (*32*) and Lancaster (*33*), Q_B^- is stabilized by 2−4 hydrogen bonds of both oxygen atoms. If one or several of these bonds cannot be established at low pH (e.g., because of an increased distance), the p*K* of Q_B^{red} will be raised and direct protonation may ensue.

Recombination Mechanism. The comparison (Figure 5) between the recombination rate vs pH curves obtained in chromatophores and isolated RCs from the same bacterium provides a striking illustration of differences, and similarities, between both materials. This rate is slower in chromatophores, whereas the Q_A^- to Q_B transfer rate is faster by a similar factor of about 3 (*9, 10*) (see footnote 7 below) which means that the native environment is better tuned for minimizing recombination. The overall shape of both curves is similar, with a marked shift of the RC curve toward acidic pH. In both instances, the recombination rate decreases when lowering the pH, until a bottom limit is attained at about 0.06−0.08 s^{-1}. The reason for this lower limit is enlightened by previous studies (*3, 34−36*) which show that the recombination involves two competing routes, either from the $P^+Q_A-Q_B$ state via the $Q_AQ_B^-/Q_A^-Q_B$ equilibrium, or directly from the $P^+Q_AQ_B^-$ state. In purified RCs from wild-type *Rb. capsulatus* or *sphaeroides*, the indirect route is dominant. However, when the equilibrium constant $K_{AB} = [Q_AQ_B^-]/[Q_A-Q_B]$ is rendered large enough (e.g., in mutants or by replacing Q_A with a low-potential quinone), the direct route from Q_B^- to P^+ can prevail. The rate constant found for this process in thus-modified isolated RCs of *Rb. sphaeroides* was in the range 0.04−0.19 s^{-1} (*3, 34−36*), consistent with the minimum rate obtained in the present study (around pH 6) of about 0.07 s^{-1} (or 0.08 s^{-1} if one only takes into account the major exponential phase). A similar low limit of 0.08 s^{-1} appears in the data of Mikšovská et al. (*22*) for RCs of *Rb. capsulatus* below pH 4 (see Figure 5). It is thus clear that in both cases the direct route becomes predominant at low pH. Due to the larger value of K_{AB} in chromatophores, the limit is attained at pH 6 instead of pH 4 in isolated RCs. In chromatophores, an increase in the rate is observed when lowering the pH below 6, which suggests that the direct recombination becomes faster when the semiquinone is directly protonated.

At pH >6, the indirect recombination path (through the equilibrium with $P^+Q_A^-$) predominates. If, as a crude approximation, one assumes negligible proton uptake by Q_A^-, the derivative of $\log(k_{BP})$ with respect to pH should reflect the extent of the uptake by Q_B^-. This would predict two peaks (for pH ≤7 and pH ≥11) for the proton uptake titration, separated by a region of low uptake in the pH 8−10 range. This is in qualitative agreement with our uptake measurements restricted to the pH 5−8.5 range. The overall shape thus predicted is roughly similar to that found in isolated reaction centers of *Rb. capsulatus* (*1*).

Electrostatic Effects. The amplitude of the electrochromic shift of Bph_B caused by Q_B^{red} around 750 nm was found to depend on pH (Figure 8). It is quite small at pH 5, as expected from the neutral character of Q_BH. The remaining change at this pH may indicate either that a small fraction of Q_B^{red} is still anionic or that the bound Q_BH still induces a dipolar moment detected by the electrochromic probe. At pH 7, the uptake of about one proton occurs although the semiquinone is not directly protonated. The net change of

[4] This does not mean that the p*K* of Q_B^{red} has to be close to its value in solution, because very large local electrostatic shifts may occur within the protein (*29, 30*).

[5] We investigated models involving Q_B interacting with one or two protonatable groups. In the latter case, for instance, one has six parameters (the intrinsic p*K*s of the two groups, the p*K* of Q_B^{red}, and three pairwise interactions between charged groups). For a given set of parameters, the pH titration of the uptake caused by Q_B reduction was computed, together with the protonation state of Q_B^{red}. Exploration of the parameter space led to the following conclusions: (i) When the experimental uptake titration is correctly mimicked, the protonation curve of Q_B^{red} displays two waves of about equal amplitudes, the high pH one accompanying the uptake titration (thus, about half the semiquinone is protonated at pH 7). (ii) When the semiquinone protonation curve is correctly mimicked, the uptake titration displays two waves, the low pH one accompanying the semiquinone reduction (thus, the uptake is about 0.5 at pH 6).

[6] We have no definite explanation for the effects of micromolar additions of ferrocene or ferricyanide that changed the pH dependence of the anionic to protonated transition. Nevertheless, they seem more easily accommodated by the idea of a conformation switch, whose pH sensitivity could be modified by the binding of these substances.

charge is thus zero, but the negative charge on Q_B^- and the positive charge of the compensating proton constitute a dipole which can exert a substantial field on the neighboring Bph. Indeed, a significant electrochromic shift is observed which, as expected, becomes larger at higher pH when the charge compensation is diminished (uptake of about 0.65 proton at pH 8.5). Extrapolation of the present data for zero proton uptake would predict roughly a doubling of the size of the signal observed at pH 7. This is still smaller than the size of the Bph_A shift caused by Q_A^- in this material [see also the Q_A^- and Q_B^- spectra obtained by Verméglio (*9*) in chromatophores of *sphaeroides* and *rubrum*], but qualitatively agrees with Tiede's view (*10*) that at short times (i.e., before the charge compensation occurs) both spectra have similar sizes. In terms of electrostatically weighted distances and assuming a linear arrangement, the bound proton would be about 2-fold more distant from Bph than Q_B^-. It should be emphasized that it may be an oversimplification to assume that the movement of charges induced by Q_B^- is strictly coupled to proton uptake. For instance, there may be proton movement within the membrane occurring faster than the uptake from the bulk (*37*), and there may even be such an internal movement (or other charge rearrangement) without any uptake. This remark also applies to the discussion of the membrane potential below.

The electrostatic effects due to proton binding in the Q_B^- region can also be studied from the carotenoid shift that reflects the delocalized membrane potential. At short times, or in the presence of stigmatellin, this signal monitors the electrogenic charge separation between P^+ and Q_A^- that spans only a fraction of the membrane width (phase A). The electron transfer to Q_B is essentially parallel to the membrane plane and thus not expected to be significantly electrogenic. Nevertheless, an increase of the membrane potential has been observed to accompany this reaction (phase BI), most probably because of the electrogenicity of proton uptake (*24*, *38*). We also observed such an increase (Figure 7) when comparing, for instance, the amplitude of the carotenoid change in the presence of stigmatellin ($P^+Q_A^-$ state) with that observed for the $P^+Q_B^{red}$ state measured a few milliseconds after the flash in the absence of inhibitor (the kinetic aspects are discussed later). The extent of this electrogenic phase increased markedly below pH 7, when direct protonation of Q_B^{red} takes place. The electrogenicity should be (assuming the uptake from the bulk accounts for all the charge compensation around Q_B^{red}) the product of proton uptake stoichiometry by the electrogenic distance spanned by the proton. From pH 7 to 5, the uptake stoichiometry is constant but the electrogenic span increases because of the direct protonation of the semiquinone. Our results may be compared with previous measurements of the electrogenicity associated with the first and second electron-transfer steps to Q_B, in chromatophores of *Rb. sphaeroides* fused with a collodion membrane (*24*). These authors found a small phase BI (about 2−3% of the amplitude of phase A in the pH range 6−8, about 7% at pH 9.5). A larger extent (15−20% of phase A) was observed on the second step ("phase BII"), when formation of Q_BH_2 implies the migration of ≥ 1 proton (i.e., the complement to 2 of the first uptake) all the way to Q_B. The average of these quantities ($B_{av} \approx$ 10%) reflects the electrogenicity of one proton transferred from the bulk to Q_B. In the present work, we obtained larger relative values for both steps. At pH 7.3, we measured about 11% for phase BI and 27% for phase BII; thus, $B_{av} = 19\%$. This quantitative discrepancy may be due to the use of a different material. On the other hand, at pH 5, we obtained typical values of 35% for both BI and BII, thus also for B_{av}, almost 2-fold the value measured at pH 7.3. Clearly, B_{av} should be constant unless the structure or dielectric properties of the RC are modified. This large increase of the relative electrogenicity associated with proton transfer to Q_B supports the possibility of a structural rearrangement occurring below pH 7. It is not possible to decide whether the increase at pH 5 of the B/A ratio is due to an increase of the B phase or to a decrease of the A phase, because the low pH caused a marked irreversible decrease of the overall field-indicating change, precluding absolute comparisons.

Electron-Transfer Kinetics. Our study of the $Q_A^-Q_B \rightarrow Q_AQ_B^{red}$ kinetics shows, in agreement with several reports (*10*, *20*, *39*), the occurrence of a fast phase ($\ll 10$ μs), followed by a slower phase in the 10−100 μs range. The fast phase is not resolved in our work, but appears as a gap between the putative origin of the kinetics ($P^+Q_A^-$ measured in the presence of stigmatellin) and the extrapolation to time zero of the slower phase, measured from 10 μs on. It must, therefore, have a half-time shorter than about 5 μs. This agrees with the determination by Tiede et al. (*10*) from absorption change kinetics in the near-infrared of $t_{1/2} \approx 2.8$ μs ($t_{1/e} \approx 4$ μs) in chromatophores of *Rb. capsulatus*. For the slow phase, these authors found in the same material at pH 7.5, $t_{1/2} \approx 28$ μs ($t_{1/e} \approx 40$ μs), which is in nice agreement with our 340 nm kinetics.[7] These results were analyzed by assigning the fast phase exclusively to electron transfer and the slow phase to charge-compensating events probably accompanied by electron transfer.

We first discuss the results obtained around pH 7.3 (Figure 6C), where the semiquinone remains anionic. The fast phase is present at 340 nm (the UV peak of the $Q_A^- - Q_B^-$ difference spectrum), where it accounts for about one-third of the total change. It is not present, however, in the kinetics of the carotenoid shift. The simplest interpretation, consistent with the results of (*20*) and (*10*), is that the electron transfer is biphasic[8] and that its slow phase is accompanied with electrogenic events (proton transfer and other local charge rearrangements). It is then tempting to assume that the electrostatic relaxation seen during the slow phase (from the carotenoid shift in the present work or from the attenuation of the BPh_B shift in Tiede's work) is in fact the driving force for the completion of the electron-transfer reaction. In other words, the initial equilibrium constant (prevailing during the fast phase) between Q_A and Q_B would be small (e.g., $K_{AB} \approx$ 0.5). The electrostatic relaxation occurring on the 10−100

[7] The $t_{1/e}$ values reported by Tiede et al. are 40 μs and 80 μs for chromatophores of *Rb. capsulatus* and *Rb. sphaeroides*, respectively (pH 7.5). For isolated RCs of *Rb. sphaeroides*, it is 208 μs. Thus, the rate is almost 3-fold slower in isolated RCs compared with membranes [in agreement with Verméglio's data (*9*)]. On the other hand, the reaction appears especially rapid in *Rb. capsulatus* compared with other species.

[8] The assumption made here is that the 340 nm change is homogeneous, rather than a mixture of one contribution monitoring only electron transfer during the fast phase and another one during the slow phase sensitive only to electrostatic changes. This assumption seems reasonable since both phases had similar spectra in the 300−350 nm region (notably an isosbestic wavelength at 320 nm).

μs time scale would then increase K_{AB} and achieve to drain the electron toward Q_B.

We now come to the results at pH 5 (Figure 6A), where the semiquinone binds a proton. The (Q_B^- − Q_BH) spectrum is maximal at 330 nm. This is a wavelength where the difference spectrum (Q_A^- − Q_B^-), with both semiquinones anionic (as measured around pH 7), is very small. Thus, at this wavelength one monitors essentially the disappearance of anionic semiquinone and the formation of the final state Q_BH. The kinetics are well described by a single exponential with $t_{1/2} \approx 15$ μs, with little unresolved fast phase between the extrapolation at time zero of this decay and the stigmatellin level. Compared with pH 7, the switch to the protonated final state has not caused any dramatic change of the rate, which is just accelerated 2-fold (in continuity with the pH dependence observed above pH 7). Although the unresolved fast phase has a small relative weight at 330 nm, it is still present with larger relative weight at other wavelengths. Due to the small signals and to the mixture with the field-indicating change (see below), it is difficult to give a definite statement, but it seems that the spectrum of this phase is similar with that of (Q_A^- − Q_B^-) as measured at pH 7. For instance, its relative amplitude (with respect to the overall change) was larger at 340 nm than at 330 nm, or at 460 nm than at 450 nm. It is thus plausible that the reaction occurs in two steps: (i) electron transfer and formation of anionic Q_B^- during the fast phase; (ii) protonation of the semiquinone during the 15 μs phase.

In contrast with the results at pH $\geq$7, there is evidence for a large fast phase ($\ll$10 μs) for the rise of the carotenoid shift at pH 5, which amounts to more than 10% of phase A (Figure 7). This may be due to a rapid electrostatic rearrangement following the electron-transfer step. Alternatively, it may be due to the electron-transfer itself. We noticed above several aspects that suggest a structural change occurring at low pH. It may then be considered that a consequence of such a change could render the electron transfer from Q_A to Q_B electrogenic. In this case, the same scheme could account for the biphasic kinetics both at pH 7 and at pH 5: (i) rapid phase of electron transfer (electrogenic at pH 5); (ii) electrostatic relaxation (with proton binding either at some distance from Q_B^- at pH 7, or directly on the semiquinone at pH 5) driving the electron transfer to completion.

We will now discuss the UV kinetics monitored on the second flash (Figures 6B,D) in the presence of a donor [second electron transfer: $Q_A^-Q_B^{red} + (2)H^+ \rightarrow Q_AQ_BH_2$]. A fast phase seems to be present in this case as well because the zero time extrapolation of the kinetics (e.g., at 340 nm for pH 7.2) was found slightly below that of the first flash, thus distinctly below the stigmatellin level. Nevertheless, the amplitude of this phase is too small to account for more than a minor fraction of electron transfer. According to the in vitro spectra published by Morrison (*27*) [see also (*40*)], among the various reduced states of ubiquinone which may be involved in the reaction, the anionic semiquinone is the only species which absorbs significantly around 330−340 nm. Therefore, the changes expected either for the reaction $Q_A^-Q_B^- + H^+ \rightarrow Q_AQ_BH^-$ or for the reaction $Q_A^-Q_B^- \rightarrow Q_AQ_B^{2-}$ correspond essentially to the destruction of two semiquinones and should be much larger than the observed rapid phase. Concerning the slow phase, which must thus include essentially all the electron transfer, a striking result is that its rate (we note it k_2) is very close to that observed for the first electron transfer (k_1), in the explored pH range (5.0−8.5). A similar result was previously reported by Verméglio (*9*) for chromatophores of *Rb. sphaeroides* in the pH range 6−10 and for isolated RCs of *Rb. sphaeroides* in the pH range 5.5−7.5 by the same author and by Wraight (*8*). There is a discrepancy between these results (in isolated RCs) and those of Kleinfeld et al. (*41*, *42*), who confirmed the rate and pH dependence found by Wraight and Verméglio (below pH 8) for k_2, but obtained a different result for k_1, namely, a constant rate below pH 8. The origin of this experimental discrepancy lies probably in the different preparation procedures used by the three groups, in particular with respect to the use of ammonium sulfate (A. Verméglio, private communication). The finding of $k_1 \approx k_2$ in chromatophores over a broad pH range (5−8.5) involving a 5-fold variation of these rates strongly suggests that a similar process is rate-limiting in both reactions. According to the analysis proposed above for the first reaction, this process involves an electrostatic relaxation that controls the driving force for electron transfer. A result from the electrostatic calculations reported by Lancaster et al. (*30*) is that the formation of Q_A^- is expected to induce proton binding by the Glu cluster near Q_B at each stage of quinone reduction, which would, as noted by the authors, "prestabilize electron transfer from Q_A to Q_B". We thus propose tentatively that, in chromatophores, the onset of this prestabilizing configuration might be the rate-limiting process in both electron-transfer steps.

It has been recently proposed that the rate-limiting step for the first electron-transfer reaction could involve a rearrangement of ubiquinone in the Q_B pocket (*32*), moving from a site incompetent for electron transfer to a site closer to His L-190 and to Q_A, where Q_B^- would be formed and remain bound until the second electron transfer. Whereas this model may be correct concerning isolated RCs, and does account nicely for the low-temperature experiments of Kleinfeld et al. (*43*), it is not plausible in the case of chromatophores, unless the similarity of k_1 and k_2 is purely coincidental. Concerning the second electron transfer, the model favored by Graige et al. (*4*) is a two-step mechanism in which fast reversible formation of the protonated semiquinone QH is followed by rate-limiting electron transfer. This model encounters the same difficulty as above to account for $k_1 \approx k_2$ in chromatophores. It would also predict a large acceleration of the rate at low pH when the semiquinone is pre-protonated, which is not consistent with the mere 2-fold acceleration observed between pH 7 and pH 5.

CONCLUSION

A number of significant differences in the functioning of the acceptor side between isolated RCs and chromatophores have been highlighted in this work and in previous literature. They concern, notably, the stoichiometry of proton uptake by Q_B^-, the faster rate of both electron-transfer reactions in chromatophores, the slower rate of $P^+Q_B^-$ recombination (and the predominance of the direct route at pH $\leq$6), and the direct protonation of the semiquinone at low pH. The origin of these differences will have to be clarified. They do not seem to imply just a different tuning of the RC

reflecting minor quantitative changes and may require the understanding of more qualitative modifications.

ACKNOWLEDGMENT

We thank A. Verméglio for guidance and very helpful advice at many stages of this work, and for reading the manuscript.

REFERENCES

1. Sebban, P., Maróti, P., and Hanson, D. K. (1995) *Biochimie 77*, 677−694.
2. Okamura, M. Y., and Feher, G. (1995) in *Anoxygenic Photosynthetic Bacteria* (Blankenship, R. E., Madigan, M. T., and Bauer, C. E., Eds.) pp 577−594, Kluwer Academic Publishers, Dordrecht.
3. Takahashi, E., and Wraight, C. A. (1992) *Biochemistry 31*, 855−866.
4. Graige, M. S., Paddock, M. L., Bruce, J. M., Feher, G., and Okamura, M. Y. (1996) *J. Am. Chem. Soc. 118*, 9005−9016.
5. Vermeglio, A. (1977) *Biochim. Biophys. Acta 459*, 516−524.
6. Hales, B. J., and Case, E. E. (1981) *Biochim. Biophys. Acta 637*, 291−302.
7. Lubitz, W., Abresch, E. A., Debus, R. J., Isaacson, R. A., Okamura, M. Y., and Feher, G. (1985) *Biochim. Biophys. Acta 808*, 467−469.
8. Wraight, C. A. (1979) *Biochim. Biophys. Acta 548*, 309−327.
9. Verméglio, A. (1982) in *Function of quinones in energy conserving systems* (Trumpower, B. L., Ed.) pp 169−180, Academic Press, New York.
10. Tiede, D. M., Utschig, L., Hanson, D. K., and Gallo, D. M. (1998) *Photosynth. Res. 55*, 267−273.
11. Jenney, F. E., and Daldal, F. (1993) *EMBO J. 12*, 1283−1292.
12. Rott, M. A., Witthuhn, V. C., Schilke, B. A., Soranno, M., Abdulfatah, A., and Donohue, T. J. (1993) *J. Bacteriol. 175*, 358−366.
13. Baciou, L., Bylina, E. J., and Sebban, P. (1993) *Biophys. J. 65*, 652−660.
14. Joliot, P., Béal, D., and Frilley, B. (1980) *J. Chim. Phys. 77*, 209−216.
15. Joliot, P., and Joliot, A. (1984) *Biochim. Biophys. Acta 765*, 210−218.
16. Rappaport, F., Blanchard-Desce, M., and Lavergne, J. (1994) *Biochim. Biophys. Acta 1184*, 178−192.
17. Dutton, P. L., Petty, K. M., Bonner, H. S., and Morse, S. D. (1975) *Biochim. Biophys. Acta 387*, 536−556.
18. Bensasson, R., and Land, E. J. (1973) *Biochim. Biophys. Acta 325*, 175−181.
19. Vermeglio, A., and Clayton, R. K. (1977) *Biochim. Biophys. Acta 461*, 159−165.
20. Li, J., Gilroy, D., Tiede, D. M., and Gunner, M. R. (1998) *Biochemistry 37*, 2818−2829.
21. Maróti, P., and Wraight, C. A. (1988) *Biochim. Biophys. Acta 934*, 329−347.
22. Miksovska, J., Kalman, L., Schiffer, M., Maróti, P., Sebban, P., and Hanson, D. K. (1997) *Biochemistry 36*, 12216−12226.
23. Jackson, J. B., and Crofts, A. R. (1971) *Eur. J. Biochem. 18*, 120−130.
24. Drachev, L. A., Mamedov, M. D., Mulkidjanian, A. Y., Semenov, A. Y., Shinkarev, V. P., and Verkhovsky, M. I. (1990) *FEBS Lett. 259*, 324−326.
25. Monger, T. G., Cogdell, R. J., and Parson, W. W. (1976) *Biochim. Biophys. Acta 449*, 136−153.
26. Brzezinski, P., Okamura, M. Y., and Feher, G. (1992) in *The Photosynthetic Bacterial Reaction Center II* (Breton, J., and Verméglio, A. Eds.) pp 321−330, Plenum Press, New York.
27. Morrison, L. E., Schelhorn, J. E., Cotton, T. M., Bering, C. L., and Loach, P. A. (1982) in *Function of quinones in energy conserving systems* (Trumpower, B. L., Ed.) pp 35−58, Academic Press, New York.
28. Hienerwadel, R., Grzybek, S., Fogel, C., Kreutz, W., Okamura, M. Y., Paddock, M. L., Breton, J., Nabedryk, E., and Mäntele, W. (1995) *Biochemistry 34*, 2832−2843.
29. Beroza, P., Fredkin, D. R., Okamura, M. Y., and Feher, G. (1995) *Biophys. J. 68*, 2233−2250.
30. Lancaster, C. R. D., Michel, H., Honig, B., and Gunner, M. R. (1996) *Biophys. J. 70*, 2469−2492.
31. Miksovska, J., Maróti, P., Tandori, J., Schiffer, M., Hanson, D. K., and Sebban, P. (1996) *Biochemistry 35*, 15411−15417.
32. Stowell, M. H. B., McPhillips, T. M., Rees, D. C., Soltis, S. M., Abresch, E., and Feher, G. (1997) *Science 276*, 812−816.
33. Lancaster, C. R. D. (1998) *Biochim. Biophys. Acta 1365*, 143−150.
34. Labahn, A., Paddock, M. L., McPherson, P. H., Okamura, M. Y., and Feher, G. (1994) *J. Phys. Chem. 98*, 3417−3423.
35. Labahn, A., Bruce, J. M., Okamura, M. Y., and Feher, G. (1995) *Chem. Phys. 197*, 355−366.
36. Allen, J. P., Williams, J. C., Graige, M. S., Paddock, M. L., Labahn, A., Feher, G., and Okamura, M. Y. (1998) *Photosynth. Res. 55*, 227−233.
37. Gopta, O. A., Cherepanov, D. A., Junge, W., and Mulkidjanian, A. Y. (1998) in *Photosynthesis: mechanisms and effects* (Garab, G., Ed.) Kluwer Academic Publishers, Dordrecht (in press).
38. Brzezinski, P., Paddock, M. L., Okamura, M. Y., and Feher, G. (1997) *Biochim. Biophys. Acta 1321*, 149−156.
39. Hienerwadel, R., Thibodeau, D., Lenz, F., Nabedryk, E., Breton, J., Kreutz, W., and Mäntele, W. (1992) *Biochemistry 31*, 5799−5808.
40. McPherson, P. H., Schonfeld, M., Paddock, M. L., Okamura, M. Y., and Feher, G. (1994) *Biochemistry 33*, 1181−1193.
41. Kleinfeld, D., Okamura, M. Y., and Feher, G. (1984) *Biochim. Biophys. Acta 766*, 126−140.
42. Kleinfeld, D., Okamura, M. Y., and Feher, G. (1985) *Biochim. Biophys. Acta 809*, 291−310.
43. Kleinfeld, D., Okamura, M. Y., and Feher, G. (1984) *Biochemistry 23*, 5780−5786.
44. Pulles, M. P. J., van Gorkom, H. J., and Verschoor, G. A. M. (1976) *Biochim. Biophys. Acta 440*, 98−106.

BI9827621